Desalination and Water Treatment
www.deswater.com

doi: 10.5004/dwt.2021.27851

242 (2021) 162–177
December

Highly competitive multicomponent adsorption of organic and heavy metals using activated mangrove charcoal

Mohamed F. Sabbagh, Muhammad H. Al-Malack*

Department of Civil and Environmental Engineering, King Fahd University of Petroleum and Mineral, Saudi Arabia, Dhahran 31261, Tel. +966138604735; Fax: +966138602789; emails: mhmalack@kfupm.edu.sa (M.H. Al-Malack), moesabbagh@outlook.com (M.F. Sabbagh)

Received 1 July 2021; Accepted 1 October 2021

ABSTRACT

Multicomponent competitive adsorption of phenol, Pb(II), Cr(III), and Cd(II) were studied using activated carbon produced from mangrove charcoal that was activated using potassium hydroxide with a specific surface area of 784 m^2/g. Effects of initial pH, adsorbent dosage, initial concentration variation, thermodynamic, and contact time were investigated. Results of the investigation showed that the maximum removal efficiency in the multicomponent system was around 76%, 92%, 47%, and 31% of phenol, Pb, Cr(III), and Cd, respectively. Those values were obtained at pH 5, adsorbent dosage of 2.5 g/L, contact time of 120 min, and an initial concentration of 50 mg/L for phenol and 30 mg/L of each heavy metal. The highest achieved adsorption capacity obtained was 46, 32, 11, and 3.8 mg/g of phenol, Pb, Cr(III), and Cd, respectively. Moreover, the results showed that the competition between phenol, Pb, and Cr(III) was fierce due to the similar adsorption mechanism. Freundlich isotherm well-fitted phenol, while Cd data were well fitted by Redlich–Peterson isotherm. On the other hand, Langmuir was found to well-fit results of Pb and Cr(III). The pseudo-second-order was the best match for the four pollutants, which indicated that chemisorption was the adsorption mechanism. Intraparticle diffusion indicated that the diffusion happened in the micro and macro levels for most of the pollutants, except for Cr(III), where it happened at the macro levels only. The thermodynamic study concluded that the nature of multicomponent adsorption was exothermic in nature, except for Cr(III), which was endothermic. Also, the highest achieved removal efficiency from the thermodynamic study was 60%, 59%, 42%, and 13% of phenol, Pb, Cr(III), and Cd, respectively at 30°C. Adsorption–desorption for the multicomponent system showed that HCl was better for heavy metals desorption due to the addition of hydrogen ions, while NaOH was better for phenol desorption due to interactions between phenol and NaOH.

Keywords: Complexation; Desorption; Industrial wastewater; Phenol; Speciation; Thermodynamic

1. Introduction

Industrial wastewater effluents typically contain streams of mixed organic and inorganic pollutants from the mining, manufacturing, petrochemical, and agriculture industry that continue to degrade water quality and contaminate the surrounding environments. Heavy metals such as chromium, cadmium, and lead continue to pose adverse effects on the health of both human beings and the environment as their toxic degradation products contribute to environmental load and harm [1,2]. Also, heavy metals bioaccumulation in the soil has proved to negatively impact the cultivated crops, where many studies have shown a very concerning high level concentration of heavy metals

* Corresponding author.

in cultivated crops, especially in lands where wastewater sludge was used as fertilizer [3,4]. Phenol and phenolic compounds pollutants form organic and free radicals that are highly reactive, which is responsible for its persistence in the environment that may pose serious health implications due to its possible carcinogenic properties [5]. Phenol and phenolic compounds are considered very toxic and have very low biodegradability [6].

Many different wastewater treatment techniques are currently available that are able to remove organics and metals. Several conventional wastewater treatment technologies were used for phenol and metals removal from industrial wastewater. For instance, membrane-based technologies are currently widely used in removing organics and inorganics; their removal efficiency depends mainly on the type of membrane used (micro-filter, ultra-filter, nano-filter, or reverse osmosis) [7]. However, membrane-based technologies are considered expensive, have high power consumption in the case of reverse osmosis (RO), and require frequent maintenance. Furthermore, another technology that is used is separation by steam distillation, which is used to isolate temperature-sensitive materials such as phenolic compounds, but it is considered an expensive method and the removal efficiency is low [7]. Among these remediation techniques, adsorption proves to be the most efficient, ease in operation, and low operation and maintenance cost method in the removal of pollutants [6]. Activated carbon which is produced from a variety of raw materials including agricultural and municipal wastes is becoming very popular to use as a low-cost biomass adsorbent. Much attention is given to activated carbon due to its availability, reusability, and low cost [8], which can be improved by methods such as chemical impregnation by different activation agents. Potassium hydroxide (KOH) has been widely used in chemical activation due to its ability to produce activated carbon with high porosity and large surface area [9]. Several studies have investigated the use of KOH as an activating agent for biomass, which usually produces activated carbon with high surface areas [10].

Numerous studies have established factors that affect the efficiency of chemically activated charcoal from waste materials in adsorbing organic and inorganic pollutants, where physical characteristics, particularly surface area and pore diameter of the KOH-activated mangrove charcoal, have been found to be proportional to the KOH concentration [11]. In aid to the optimization of the physical characteristics of activated charcoal via chemical treatment, operating parameters including pH, dosage, temperature, and contact time have also been established and well-documented to affect adsorption efficiency [12,13]. Pal et al. [14] investigated the removal of ethanol using activated carbon derived from mangrove modified with KOH, where he studied the adsorption under various temperatures. Ngugi et al. [15] studied the removal of lead ions using unmodified powdered mangrove roots, the study demonstrated that the removal increased with the increase of pH and adsorbent dosage. Furthermore, several studies have investigated the removal of lead using mangrove, most of these papers attributed the adsorption of lead ions to the interaction with the carbonyl and hydroxyl functional groups acting on the adsorbent surface [16]. Adsorption has been widely used in removing heavy metals, Anwar et al. [17] studied the adsorption of lead and cadmium using a banana peel, his study concluded that pH, adsorbent concentration, and agitation speed were the important factor that affected the adsorption process. Fahim et al. [18] investigated the removal of Cr(III) using activated carbon derived from sugar industrial waste, the study reported that the maximum adsorption capacity achieved was at pH 5, because Cr(III) in strong acidic media appear as Cr(III), while in pH 5 the dominant species were $Cr(OH)^{2+}$.

In this study, KOH-activated carbon derived from mangrove charcoal was investigated for its adsorptive capacity for removing simultaneously phenol, cadmium, chromium(III), and lead together in one batch. Additionally, an investigation of desorption efficiency was also employed for the optimization of recovery methods and regeneration potentiality. The study is a novel contribution to research surrounding the feasibility of multicomponent adsorption by KOH-activated mangrove charcoal with thermodynamic and regeneration investigation, in order to model a real-life problem, which is the removal of mixed organic and inorganic pollutants from aqueous systems and to understand the interaction between pollutants on the adsorption process. Up to the knowledge of the authors, no research has been done on the use of activated carbon derived from mangrove charcoal to remove phenol, chromium(III), and cadmium in a singular batch. Moreover, very few and limited studies have investigated the removal of lead using activated mangrove charcoal. Furthermore, no research has been conducted on the removal of multi-pollutant together in one batch with thermodynamic and regeneration studies.

2. Materials and methods

2.1. Materials

Commercial mangrove charcoal was collected, oven-dried overnight at 105°C, washed to remove dirt, and oven-dried again at the same temperature and duration. Consequently, the dried mangrove charcoal was crushed and sieved to 2 mm particle size before being stored in glass containers. Chemical materials that were utilized in this research were all of the analytical grades and include the following; lead nitrate salt $Pb(NO_3)_2$ (≥99%) and cadmium nitrate salt $Cd(NO_3)_2{\cdot}4H_2O$ (≥98.5%) (VWR BDH Chemical Ltd, US, Pennsylvania), chromium chloride $CrCl_3$ (≥98%), hydrochloric acid HCl (34%–37%), and sodium hydroxide NaOH (98%) (Fischer, US, Massachusetts), phenol crystals (≥99.9%) and potassium hydroxide pellets KOH (≥85%) (Sigma-Aldrich, US, Missouri).

2.2. Activated charcoal production

Dried mangrove charcoal was thoroughly mixed with KOH pellets using a 3:1 (KOH: charcoal) ratio. Impregnated charcoal samples were oven-dried at 110°C for 12 h to remove excess moisture. The dried samples were inserted in stainless steel pipes with two narrow port diameters. The impregnated dried charcoal sample-packed stainless steel tubes were then placed in a furnace (Nabertherm LT

5/12, Germany) and heated to 600°C temperature with a heating rate of 10°C/min for 1 h. After heating, the tubes were taken out from the furnace after reaching the desired holding time. Subsequently, and in order to remove residuals, activated charcoal samples were cooled and washed continuously with de-ionized water, till the pH of the rinse water approached a pH value between 6.5 and 7.5. Finally, wet activated charcoal samples were oven-dried at 105°C for overnight and stored in glass containers.

2.3. Analytical techniques

Phenol quantification was carried out using UV-Vis Spectrometer (Shimadzu, Japan), while heavy metals quantification was carried out using Atomic Absorption Spectroscopy, AAS (PerkinElmer 700, USA) through the direct air-acetylene flame method.

Eqs. (1) and (2) were implemented to quantify the removal and the adsorption capacity, respectively.

$$q_t = \frac{\left(C_o - C_t\right)V}{m_0} \tag{1}$$

$$\text{Removal efficiency}\left(\%\right) = \frac{C_o - C_t}{C_o} \times 100 \tag{2}$$

where q_t is the amount of pollutants adsorbed (mg) per adsorbent (g); C_o (mg/L) is the initial concentration of adsorbate; C_t (mg/L) is the final concentration of adsorbate; V (L) is the volume of solution; M (g) is the mass of adsorbent.

2.4. Adsorption experiments

The adsorption experiments have been conducted in a batch mode. Erlenmeyer flask with 200 mL capacity was used and filled with 100 mL solution with certain concentrations of phenol, Pb, Cd, and Cr(III). The experiments were conducted at room temperature almost 25°C, except for the thermodynamic study. The samples were placed on an orbital shaker with 250 rpm speed to ensure that solutions were well-mixed with the adsorbent. The adsorption isotherm models of Langmuir, Freundlich, Temkin, and Dubinin–Radushkevich were used to fit the experimental data obtained from the equilibrium experiments. Also, the kinetic models pseudo-first-order, pseudo-second-order, and intraparticle diffusion were used to fit the experimental data obtained from the kinetic experiments, which account for the physisorption, chemisorption, and diffusion mechanisms, respectively, and are defined by linear Eqs. (7)–(9).

2.4.1. Langmuir isotherm

The Langmuir isotherm defines the surface coverage of adsorption and desorption in dynamic equilibrium using linear Eq. (3), where C_e is the equilibrium concentration in a liquid phase, q_e is the equilibrium concentration in a solid phase, and q_m and K_L are Langmuir constants relating to adsorption capacity [19].

$$\frac{C_e}{q_e} = \frac{1}{K_L q_m} + \frac{C_e}{q_m} \tag{3}$$

2.4.2. Freundlich isotherm

The Freundlich isotherm model defines the surface heterogeneity and exponential distribution of active sites and their energies using linear Eq. (4), where K_F is the Freundlich constant relating to adsorption capacity and 1/n is the adsorption intensity [19].

$$\log q_e = \log K_F + \frac{1}{n}\log C_e \tag{4}$$

2.4.3. Redlich–Peterson isotherm

The Redlich–Peterson isotherm is a combination between Langmuir and Freundlich isotherms. The model describes the adsorption mechanism as a mix and it does not follow an ideal monolayer system. The isotherm is represented by Eq. (5), where A is Redlich–Peterson isotherm constant, and β is constant [19].

$$\ln\frac{C_e}{q_e} = \beta \ln C_e - \ln A \tag{5}$$

2.4.4. Temkin isotherm

The Temkin isotherm model defines the effect of adsorbate interactions, assuming that the heat of adsorption decreases with increased surface coverage. The isotherm is represented by Eq. (6), where b is the heat of sorption, R is the universal gas constant, and K_T is the Temkin isotherm constant [19].

$$q_e = \frac{Rt}{b}\ln K_T + \frac{RT}{b}\ln C_e \tag{6}$$

$$B_T = \frac{RT}{b}$$

2.4.5. Dubinin–Radushkevich isotherm

The Dubinin–Radushkevich (D-R) isotherm model defines adsorption mechanism with Gaussian energy distribution on heterogeneous surfaces and is usually used to differentiate the physical and chemical adsorption of metal ions in varying temperatures. The isotherm is represented by Eq. (7), where q_D is theoretical adsorption capacity at saturation, B_D is the isotherm constant, T is the absolute temperature in Kelvin, and E is the mean adsorption energy [19].

$$\ln q_e = \ln q_D - 2B_D RT \ln\left(1 + \frac{1}{C_e}\right)$$
$$E = \frac{1}{\sqrt[2]{2B_D}} \tag{7}$$

2.4.6. Pseudo-first-order kinetic model

The pseudo-first-order model represents the physical interaction adsorption mechanism, the following equation represent the linearized form of pseudo-first-order:

$$\log\left(q_e - q_t\right) = \log\left(q_e\right) = \frac{K_1 t}{2.303} \tag{8}$$

where q_e is the equilibrium adsorption capacity, K_1 is the pseudo-first-order constant rate, t is the time in minutes, and q_t adsorption capacity [20].

2.4.7. Pseudo-second-order kinetic model

The pseudo-second-order model represents the chemical interaction adsorption mechanism, the following equation represent the linearized form of pseudo-second-order:

$$\frac{t}{q_t} = \frac{1}{K_2 q_e^2} + \frac{t}{q_e} \tag{9}$$

where q_e is the equilibrium adsorption capacity, K_2 is the pseudo-second-order constant rate, t is the time in minutes, and q_t adsorption capacity [20].

2.4.8. Intraparticle diffusion kinetic model

The intraparticle diffusion model suggests that the intraparticle diffusion will take place in the adsorption if the plot of q_t against the square root of time was linear, the following equation represents the intraparticle diffusion model:

$$q_t = k_i t^{1/2} + C \tag{10}$$

where q_t is the adsorption capacity, k_i is the intraparticle diffusion constant, t is the tie in minutes, and C is the linear intercept [20].

2.5. Regeneration

The regeneration investigation was performed according to the following procedure: (1) exhausted activated carbon (AC) samples were washed with de-ionized water to remove excess pollutants, (2) AC samples were dried to remove excess moisture, (3) dried AC samples were placed in a conical flask with 5 N of NaOH or HCl and placed on the shaker for desorption for 2 h, (4) obtained AC samples were washed thoroughly with de-ionized water to reach neutral pH, (5) washed AC samples were dried and used for another cycle of adsorption. Because of the careful procedure that was adopted, the adsorbent weight loss was minimal and did not exceed 10%.

2.6. Thermodynamic

The effect of temperature on the adsorption process was studied using the following technique: The flask was placed inside a beaker and submerged in water to ensure adequate heat distribution, then the beaker was placed on a magnetic stirrer with a temperature and speed controlling function. Also, a thermometer was placed inside the flask throughout the experiment to make sure that the temperature was constant.

3. Results and discussion

3.1. Multicomponent adsorption experiments

3.1.1. Effect of pH

The investigation of pH is very important since adsorption is heavily dependent on this parameter. The importance of pH comes from its influence on the element behavior and the ionization degree. In order to better understand the pH effect, Visual MINTEQ 3.1 software was implemented to understand the speciation of the adsorption components together. Fig. 1 shows the speciation of phenol (50 mg/L), Pb (30 mg/L), Cr (30 mg/L) and Cd (30 mg/L) at 25°C. Fig. 1a clearly shows that phenol and Cd are very stable at pH values ranging from 1 to 8, where phenol, at this pH range, appears in the undissociated form. However, for Pb, the change occurs between pH 6 and 7, where the Pb starts to precipitate in the form of PbOH. Similar results were reported by Wang et al. [21], who studied the Pb speciation. Finally, Cr is the most unstable element in the diagram, where the transformation starts at pH 3 when it reacts to form $CrOH^{+2}$. Similar results were reported by Liu et al. [22] who studied the adsorption behaviors of Cr(III) and Cr(IV) onto kaolin.

The influence of pH on the adsorption of the multicomponent system was examined by changing the pH and fixing the other parameters. Adsorbent dosage was fixed at 1.25 g/L, contact time at 2 h, and initial concentration was fixed at 50 mg/L for phenol and 30 mg/L for the heavy metals. Fig. 2 shows that the effect of pH on the phenol removal was insignificant, where the fluctuations were very small and varied between 69% and 73%. This phenomenon is attributed to the fact that phenol at pH ranges from 1 to 7 present in the undissociated form non-ionized state [23]. As shown in Fig. 1, diffusion adsorption will be favorable, rather than charge interaction. According to Xie et al. [24] who investigated the adsorption of phenol using commercial AC, pH between 5 and 7 is the best pH range for phenol adsorption due to the minimal electrostatic repulsion. The effect of pH on the removal of Pb in the multicomponent system can be seen in Fig. 2. The figure clearly shows that adsorption of Pb was significantly influenced by pH values, where Pb removal was found to increase from 16% to 73% when the pH value was increased from 2 to 5. This could be attributed to the reduced competition of hydrogen ions at higher pH [25–27]. Moreover, it can be seen from Fig. 1c that Pb at pH 5 was in the Pb form and in the transition phase because at pH 6 it started to transform to PbOH. Moreover, cadmium was slightly affected by pH variation, where the removal was 2.2% at pH 2 and 8% at pH 5. This could be attributed to the fact that Cd was still in a very stable condition, based on the speciation diagram, and the slight increase was due to the reduced competition from hydrogen ions at pH 5. Similar findings were reported by Al-Malack and Dauda [28] who investigated the removal of Cd and phenol using activated sludge waste. They reported that when the pH was increased, the removal of Cd was found to increase due to the reduced hydrogen presence

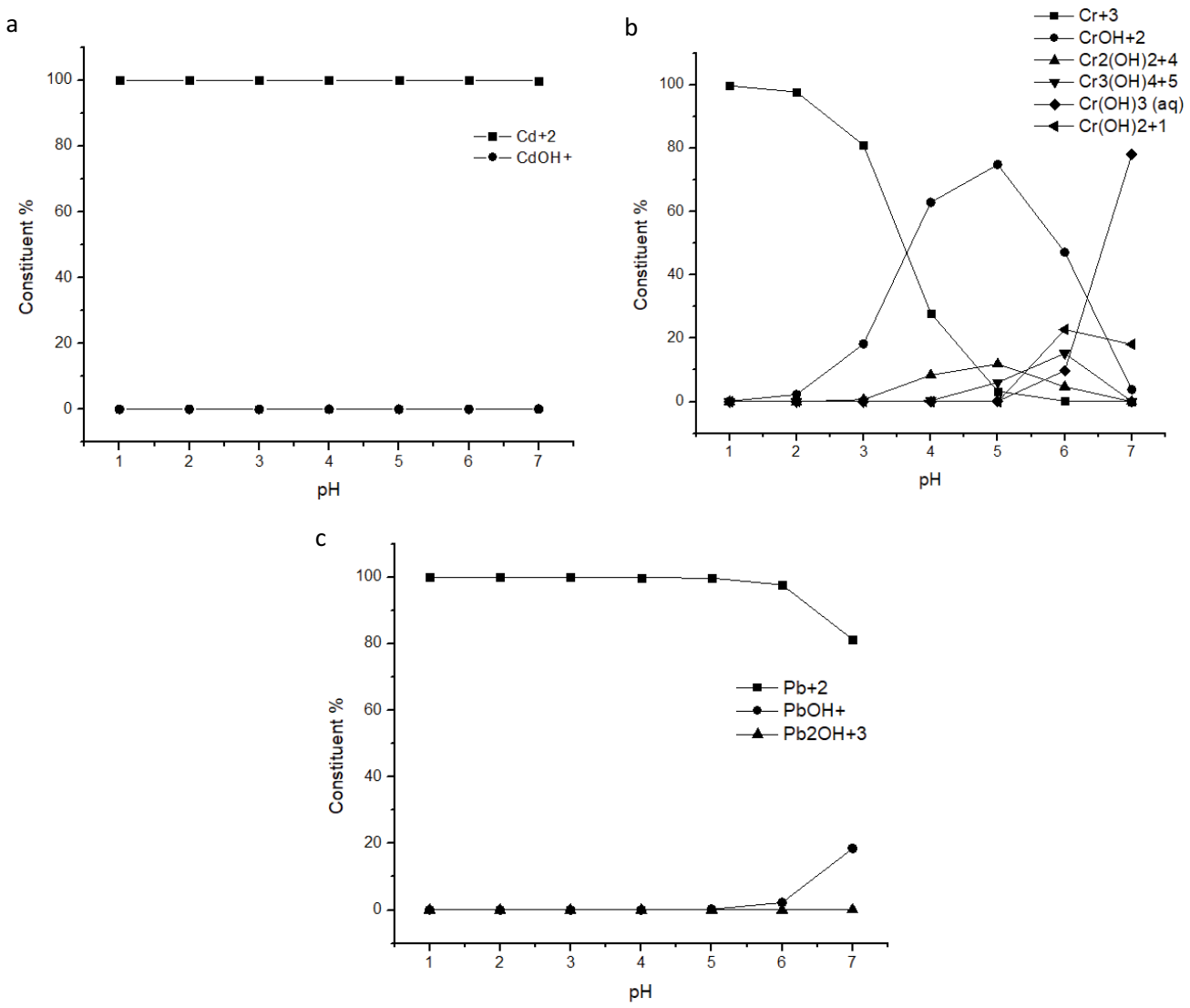

Fig. 1. Speciation diagram for the multicomponent system: (a) Cd, (b) Cr3, and (c) Pb.

at higher pH values. Arcibar-Orozco et al. [29], who studied the removal of Cd and phenol by adsorption, reported that the presence of phenol decreased the intake of Cd due to the steric hindrance for cations to adsorb specific oxygenated groups. Furthermore, the figure shows that Cr(III) adsorption was strongly impacted by the change of pH, where the removal increased by 24% when pH values were increased from 2 to 5. Fig. 1 shows that Cr(III) speciation changed rapidly with the pH change and at pH 5 chromium was in cation Cr(III) and $CrOH^{2+}$ forms. The increase in the removal was attributed to the preference of the AC to adsorb Cr in the hydrolyzed form rather than unhydrolyzed form [22]. Mohamed et al. [30] who studied the removal of Cd and Cr(III) using *Padina gymnospora* waste, reported that the increase of pH had a positive impact on the removal of Cr(III) because of the protonation assay of the adsorbent surface at the acidic media. Moreover, Alemu et al. [31] reported that the removal of Cr(III) increased with the increase of pH, which was attributed to the Cr^{3+} complexation in the aqueous solution that reduced the repulsion of cations. Several studies have reported that adding an organic compound to an aqueous solution that contains heavy metals increases the removal efficiency of the metals [32,33]. However, these findings contradict with the obtained results shown in Fig. 2 that might be attributed to the organic compound (phenol) in the current experiment was in the undissociated form as shown in the speciation diagram in Fig. 1, which might have prevented the complexation between phenol and the heavy metals. It can be concluded that the presence of phenol, Pb, Cd, and Cr(III) in one system did not alter their behavior with respect to pH variation.

3.1.2. Effect of adsorbent dosage

Effects of adsorbent dosage on the multicomponent adsorption were investigated, where the investigated dosages were 0.5, 1.25, 2, and 2.5 g/L. Batch experiments were

conducted under the following conditions: pH value of 5 (optimum), initial concentration of 50 mg/L of phenol, 30 mg/L of heavy metals, and contact time of 120 min.

Fig. 3a shows that the variation of the adsorbent dosage highly influenced the removal efficiency of the pollutants in the multicomponent system. Lead removal was found to increase from 53% to 92% when the AC dosage was increased from 0.5 to 2.5 g/L. Moreover, phenol intake was found to increase from 42% to 76%, when the adsorbent dosage was increased. It was noted that, for phenol, the difference in the removal between 2 and 2.5 g/L was slight, which might be attributed to the AC that had a higher affinity towards Pb since Pb removal kept on increasing at the same range. Chromium removal was also found to increase from 17.6% to 46.6% when the adsorbent dosage was increased, however, it reached a stability point between 2 and 2.5 g/L since the increase at that range was minimal. Finally, cadmium intake was significantly affected by the increase of AC dosage, the removal was found to increase from 5% to 32%. The increase in the removal, when the dosage was increased in the multicomponent system, was due to the increase of the available site for adsorption and to the higher contact chance between the AC and the pollutant [34]. Fig. 3b shows the effect of increasing the adsorbent dosage on the adsorption capacity. It can be noted that when the adsorbent dosage was increased, the adsorption capacity was found to decrease. Phenol adsorption capacity was found to decrease from 46 to 15.2 mg/g when the adsorbent dosage was increased from 0.5 to 2.5 g/L. A similar trend can be found with the other heavy metals, except for cadmium where there was a slight increase when the adsorbent dosage was increased, where the adsorption capacity increased from 3 to 4 mg/g. This event might be due to the unsaturation effect of adsorption sites that happens because of using high AC doses while fixing the initial concentration of the pollutants [35]. However, at lower AC dosages, the chances of the adsorption sites being fully saturated are higher due to the limited available sites.

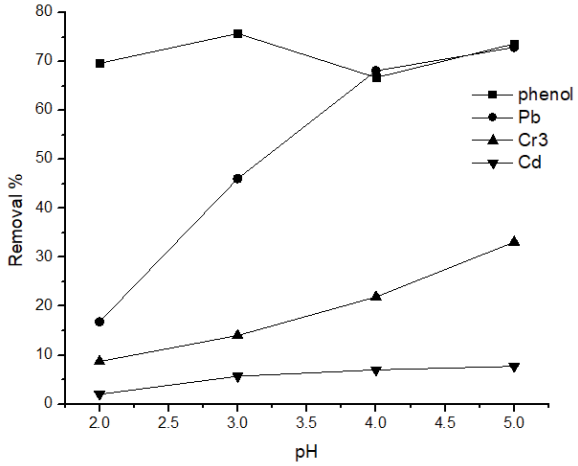

Fig. 2. Effect of pH on the multicomponent adsorption.

3.1.3. Effect of contact time and heavy metal initial concentration variation on phenol adsorption

The effect of the initial concentration of heavy metals on phenol removal was investigated by fixing the concentration of phenol and changing metal concentration. Several parameters were fixed, namely, pH (5), adsorbent dose (1.25 g/L), and phenol initial concentration (50 mg/L). As mentioned before, initial experiment o phenol removal in the presence of Pb, Cd, and Cr(III) in singular systems with the same fixed parameters (pH, adsorbent dose, and phenol concentration) were performed. The results can be seen in the Supplementary Materials, where removal efficiencies were 81%, 97%, 60%, and 47% for phenol, Pb, Cr(III), and Cd, respectively. It is worth mentioning that the Fourier-transform infrared spectroscopy results can also be found in the Supplementary Materials.

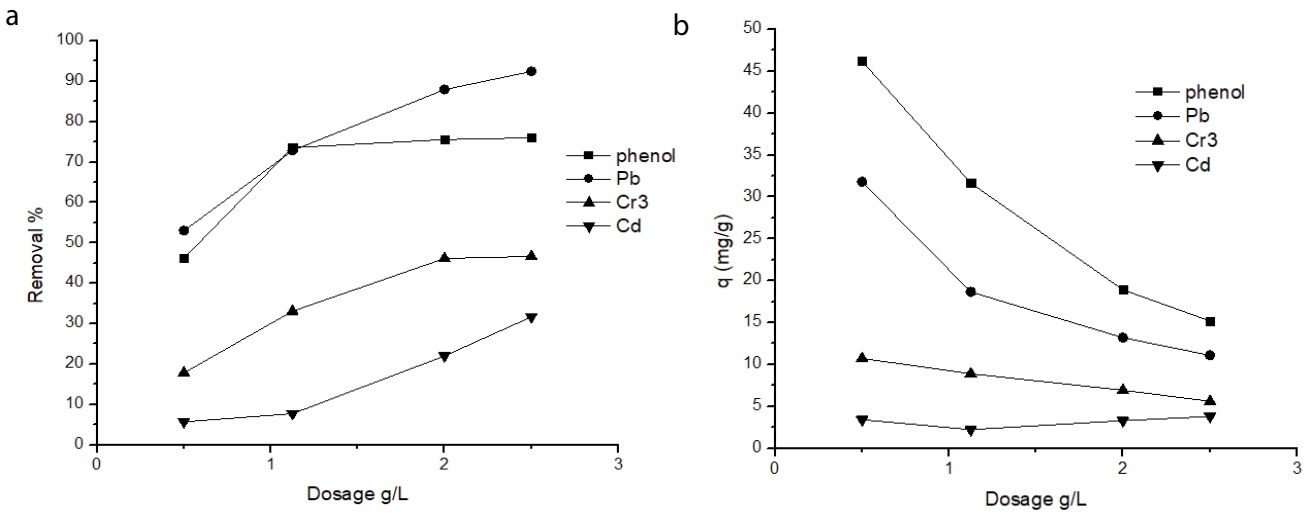

Fig. 3. Effect of the adsorbent dosage variation on the adsorption of the multicomponent system (a) removal efficiency and (b) adsorption capacity.

Fig. 4 shows that the removal efficiency of phenol was the highest when compared to the metals. When the heavy metal concentrations were 30 and 50 mg/L, phenol removal efficiency was not found to be significantly affected, when compared to the singular adsorption experiments, where the drop was around 10%. However, when heavy metals concentrations were increased to 100 mg/L, the drop in phenol adsorption was around to be 20%, where the removal efficiency of phenol reached 50% that is considered a significant drop. This behavior might be due to the fact that the increase in heavy metals concentrations resulted in fierce competition for the limited sites on the AC surface. The removal of Pb at the beginning of the adsorption experiment was high and then started to decrease, which indicates that Pb adsorption in this system was unstable due to competition from phenol and Cr(III). From the results, it can be noted that the decrease in Pb removal with time accompanied an increase in phenol and Cr(III) removal efficiencies, which might be attributed to the competition between phenol and Pb on the interaction of the carbonyl group on the AC surface. The removal of Cd was the lowest among the other pollutants, which implies a low affinity to the material. Karnib et al. [36] who studied the removal of several heavy metals using activated carbon reported that the adsorption of the heavy metals decreased with the increase of the heavy metal initial concentration, which was due to the adsorption of heavy metals on the activated carbon that occurs on a specific site. Therefore, any increase in the initial concentration without increasing the dosage causes a decrease in the removal efficiency, which explains the competition between lead and chromium. Furthermore, Duan et al. [37] reported that the adsorption of heavy metals heavily depends on the type of utilized AC, and the most common adsorption mechanisms of heavy metals onto activated carbon were surface complexation, ionic exchange, and electrostatic interaction.

3.1.4. Effect of initial concentration variation of phenol with fixed heavy metal

The effect of phenol initial concentration variation on the adsorption process was investigated, where heavy metals initial concentrations were fixed at 50 mg/L. Fig. 5a shows that when phenol concentration was lower than the concentration of heavy metals, the removal of phenol was low when compared to results obtained when phenol concentration was increased, as can be seen in Fig. 5b. This can be attributed to the mass transfer phenomena and the presence

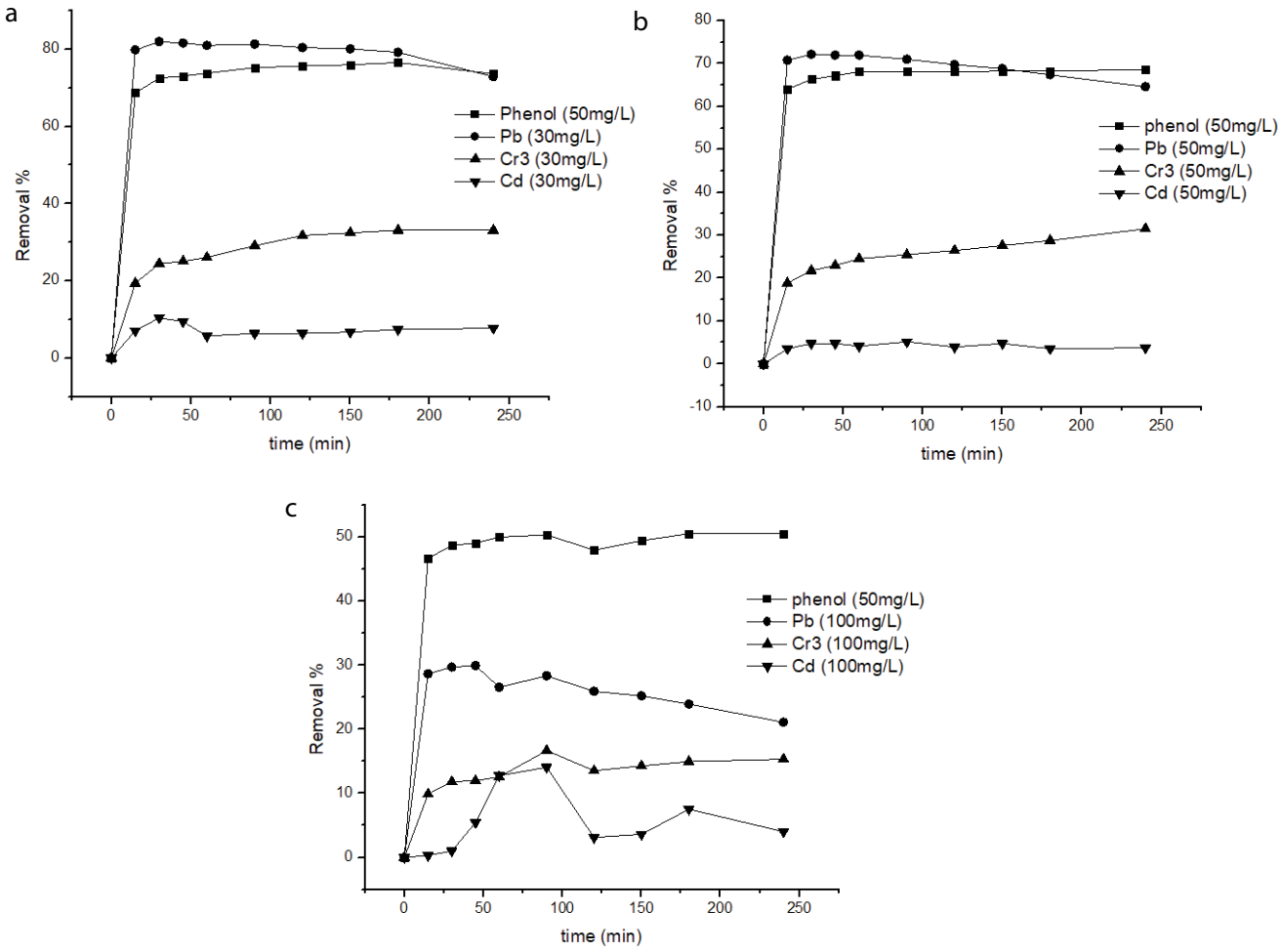

Fig. 4. The effect of heavy metals initial concentration variation on the adsorption in multicomponent system.

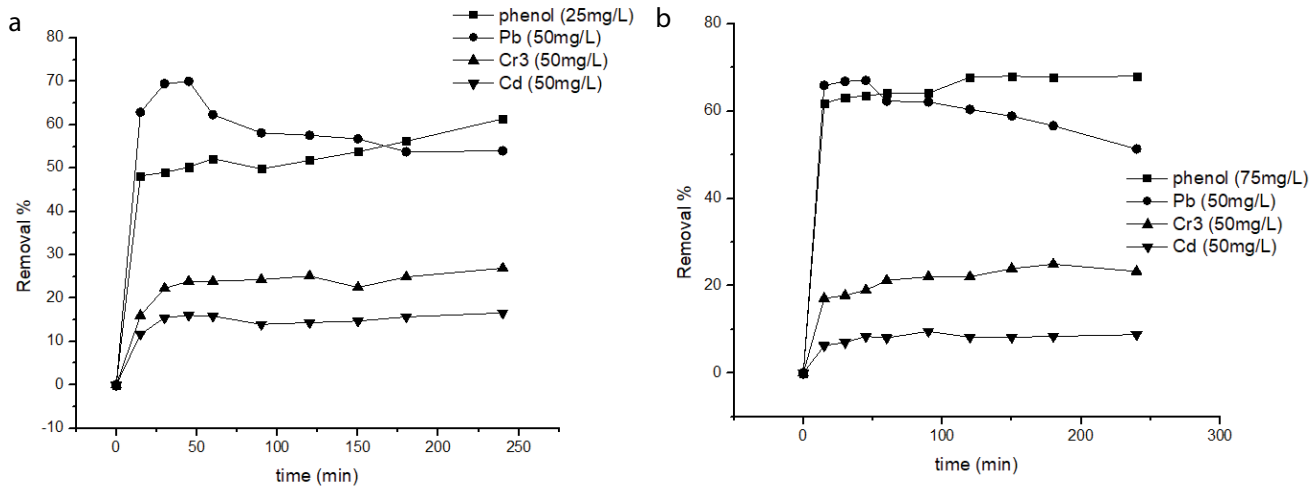

Fig. 5. The effect of phenol initial concentration variation on the adsorption in multicomponent system.

of some sites exchange between Pb and phenol. Fig. 5b shows that when phenol concentration was increased to 75 mg/L, the adsorption of phenol was more stable than the results presented in Fig. 5a. Phenol removal with three heavy metals at an initial concentration of 75 mg/L was almost similar to phenol removal that was presented in Fig. 4b. Similarly, the removal of phenol presented in Fig. 5b was higher than presented in Fig. 5a, which can be attributed to the higher mass transfer rate. Moreover, when phenol concentration was high, it facilitated contact with the AC surface. Similar results were reported by Fu et al. [38], who investigated the removal of phenol using activated carbon derived from rice husk. They reported that the removal of phenol occurs by diffusion, which explains the increase in the removal of phenol when the initial concentration was increased.

3.1.5. Adsorption equilibrium isotherms

The obtained experimental results from the multicomponent adsorption were fitted using Langmuir, Freundlich, Redlich–Peterson, Temkin, and D-R isotherms. Parameters of the models can be found in Table 1, where the parameters were obtained from Fig. 6.

It can be observed from Table 1 that Freundlich, Langmuir, Redlich–Peterson, and Temkin isotherms well fitted the results of phenol, based on the correlation coefficient. However, the negative value of K_T, which is the adsorption energy, indicates that the nature of the adsorption is endothermic, which contradicts the obtained results in the thermodynamic study in section 3.3. Also, the calculated q_m obtained from the Langmuir model did not match the maximum experimental q which was 30.24 mg/g. For Pb, Langmuir, Redlich–Peterson, and D-R isotherms well fitted the obtained results. Furthermore, Langmuir isotherm gave a correlation coefficient of 0.99 and a calculated q_m of 20.7 mg/g, which is close to the experimental q_e (19.92 mg/g). Also, the β obtained from the Redlich–Peterson isotherm was 0.82 which indicates favorable adsorption. Nevertheless, for the D-R isotherm, the correlation coefficient obtained was 0.93 and the mean energy E obtained was 35.3 J/mol that is less than 8 kJ/mol, which indicates that the adsorption is physical adsorption that contradicts the results obtained from the kinetic study. In the case of Cr(III), based on the correlation coefficient, Langmuir and Redlich–Peterson isotherm model well fitted the data. Additionally, the calculated q_m was close to the q_e experimental, which was 10.24 mg/g. Finally, the five isotherms well fitted the data of Cd based on the correlation coefficient. Though Langmuir did not accurately predict the experimental q_e and D-R isotherm gave an E value less than 8 kJ/mol that indicated physical adsorption, which contradicts the findings obtained from the kinetic study. However, Temkin isotherm had a positive value for the adsorption energy K_T, which indicates exothermic nature, which agrees with the finding in the thermodynamic study. In conclusion Temkin and Redlich–Peterson isotherm both well fitted the results of Cd in the multicomponent system. It is worth mentioning that there is a lack of information in the published literature on isotherm studies that have been conducted on the removal of phenol in the presence of metals, particularly, Pb, Cd, and Cr(III).

3.1.6. Adsorption kinetics

Experimental data on adsorption kinetics for a multicomponent system has been fitted into pseudo-first and second-order models and intraparticle diffusion. The kinetic model is a very crucial indicator of the adsorption mechanism and important data for large-scale uses. Eqs. (8)–(10) were used.

Fig. 7 shows the plot for pseudo-first and second-order models and intraparticle diffusion, while Table 2 shows the most important model parameters. As shown in Fig. 7a, the pseudo-first-order model didn't fit the experimental results, except for Cr(III), which has a correlation coefficient of 0.89, however, the calculated q_e was higher than the experimental q_e. It can be noted from Fig. 7b that pseudo-second-order model fitted well all the pollutant adsorption experimental results. Furthermore, from Table 2, all the correlation coefficients were between 0.98 and 1, and

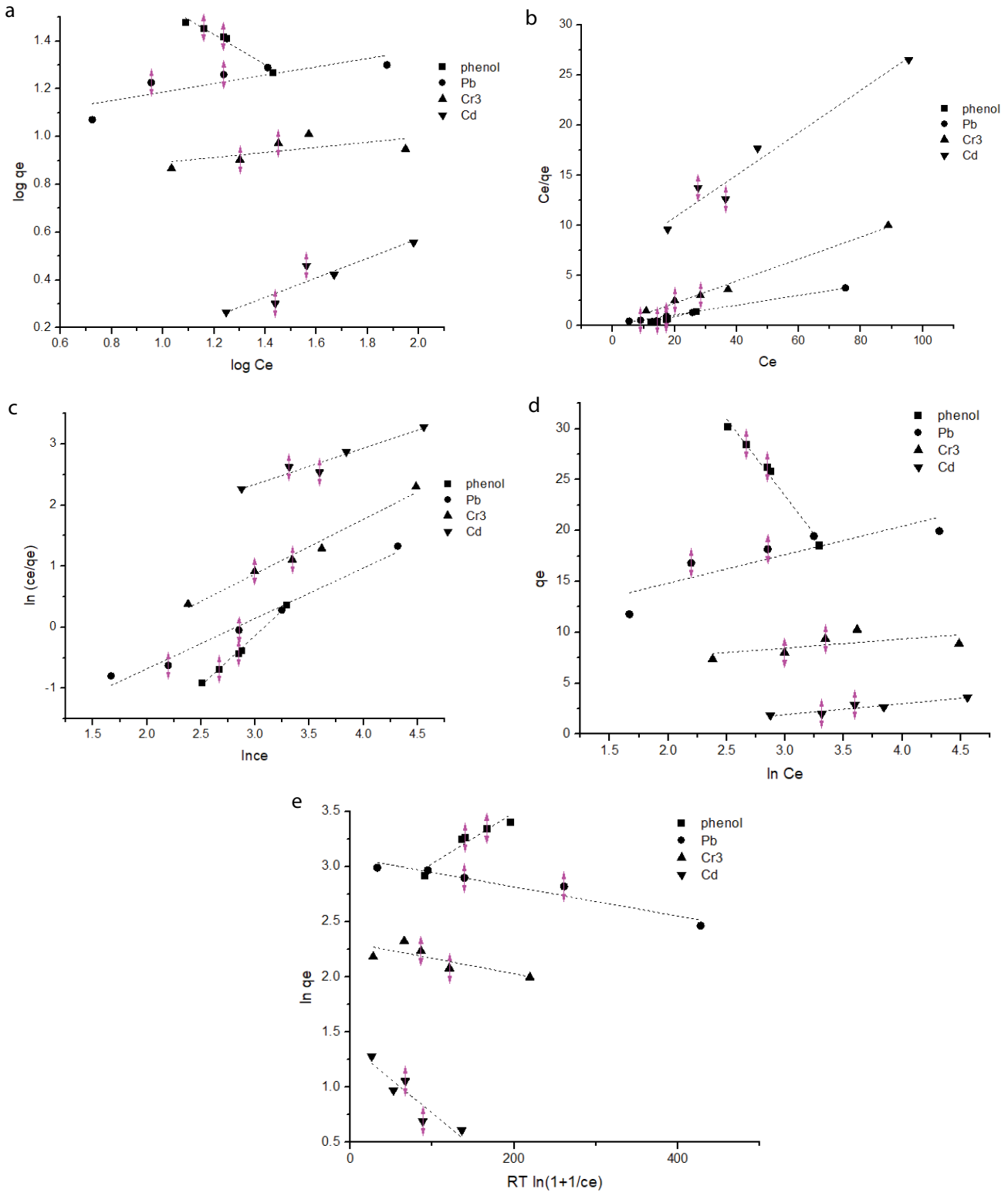

Fig. 6. Adsorption isotherms (a) Freundlich, (b) Langmuir, (c) Redlich–Peterson, (d) Temkin, and (e) Dubinin–Radushkevich.

the q_e calculated was very close to the q_e obtained by the experimental analysis. Moreover, since pseudo-second-order model well fitted all the obtained experimental data for the four pollutants, which indicates that the adsorption mechanism was chemisorption. However, it can be noted that the adsorption in the multicomponent system was not stable and did not reach equilibrium at a fast rate. The intraparticle diffusion model gives an indicator of whether the

Table 1
Important isotherms parameters

Pollutant	Freundlich model parameter			Langmuir model parameter		
	n	K_F (mg/g)	R^2	q_m (mg/g)	K_L (L/mg)	R^2
Phenol	1.59	152.4	0.963	13.67	0.13	0.98
Pb	5.67	10.2	0.7	20.7	0.38	0.99
Cr	9.41	6.1	0.4	9.1	2.2	0.99
Cd	2.44	1.76	0.89	4.73	0.03	0.96
	Redlich–Peterson model parameter					
	A (L/g)		β (L/mg)		R^2	
Phenol	152.69		1.63		0.99	
Pb	10.23		0.82		0.98	
Cr	6.1		0.89		0.98	
Cd	1.76		0.59		0.94	
	Temkin model parameter			Dubinin–Radushkevich model parameter		
	B_T	K_T (L/mg)	R^2	B_D (mol²/J²)	q_D (mg/g)	E (J/mol) – (R^2)
Phenol	–15	95.28	0.98	0.0023	13	14.74–0.9
Pb	2.8	27.06	0.75	0.0065	21.78	8.77–0.93
Cr	0.89	687.4	0.37	0.0007	10.1	26.73–0.62
Cd	1.1	3.36	0.89	0.0031	3.95	12.7–0.85

diffusion occurred at the micro or macropores level [39]. Fig. 7c shows that the adsorption happened in two stages for phenol cadmium and lead, which indicates that the adsorption happened in the micro and macropores, however, chromium adsorption occurred at the first stage in macropores.

3.2. Scanning electron microscopy and energy-dispersive X-ray spectroscopy of loaded activated charcoal

Scanning electron microscopy (SEM) and energy-dispersive X-ray spectroscopy (EDS) was conducted on the activated charcoal after adsorption to prove that the adsorption occurred on the AC surface, where Fig. 8 shows the SEM/EDS results after the multicomponent adsorption. It can be observed, from the EDS table, the presence of phenol in the form of C and O and Pb and Cr(III) can be also found. Cadmium could not be identified due to the low removal compared to the other elements. In summary, surface spot elemental constituents EDS analysis confirmed the transfer of phenol, Cr(III), and Pb from aqueous solutions to the activated charcoal surface.

3.3. Thermodynamic

The effect of temperature on the adsorption of phenol and heavy metals in the multicomponent system was investigated at the following different temperatures (30°C, 45°C, and 60°C). The conditions were fixed as the following: pH of 5, phenol concentration of 50 mg/L, heavy metals concentration of 30 mg/L, and adsorbent dosage of 1.25 g/L.

It can be observed in Fig. 9a that there was a very slight change in the removal after increasing the temperature from 25°C to 30°C, when compared to the results presented in Fig. 4. However, Fig. 9b clearly shows the reduction in the removal of phenol and lead from 68% at a temperature of 30°C to 60%, when the temperature was increased to 45°C, however, there was an increase of about 8% in the case of chromium. Finally, it can be observed from Fig. 9c that when the temperature was increased to 60°C, the removal of phenol and Pb dropped again with lead reduction was the most significant. These results indicate that the adsorption experiment was exothermic, which means that any increase in the temperature accompanies a decrease in the adsorption capability.

The following equations were used to determine free energy (ΔG°), enthalpy (ΔH°), and entropy (ΔS°):

$$\Delta G = -RT\ln K_d \tag{11}$$

where R = 8.314 J/mol K, K = temperature in Kelvin, K_d = equilibrium constant.

$$K_d = \frac{C_{ae}}{C_e} \tag{12}$$

where C_{ae} (mg/L) is the concentration of the pollutant on the activated carbon at the equilibrium and C_e (mg/L) is the concentration of the pollutant in the solution at the equilibrium. Enthalpy (ΔH), free energy (ΔG), and entropy (ΔS) were calculated using the following relationship:

$$\ln\left(K_d\right) = \left(\frac{\Delta S}{R}\right) - \left(\frac{\Delta H}{RT}\right) \tag{13}$$

Table 3 shows the calculated free energy, entropy, and enthalpy, where free energy has been calculated from

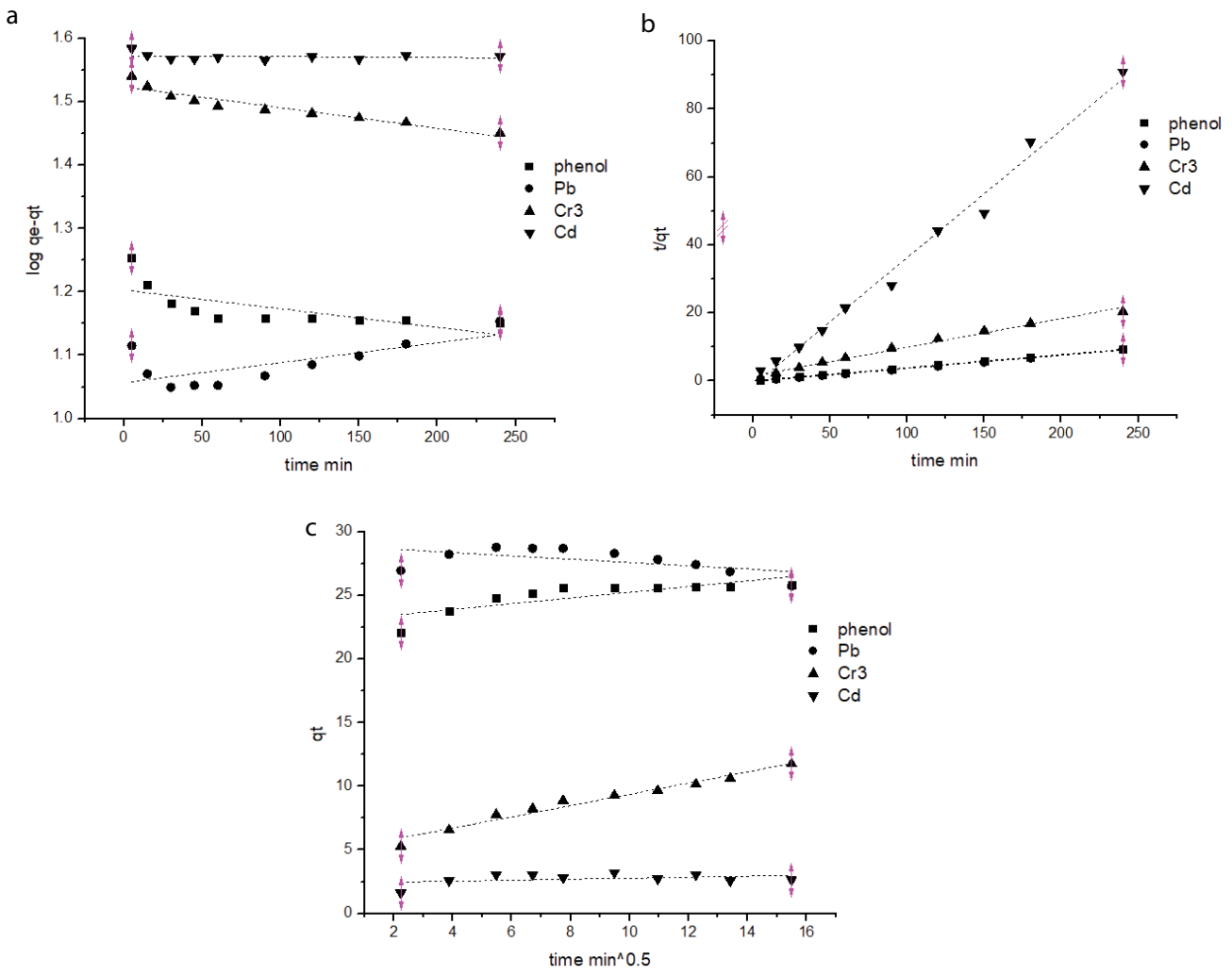

Fig. 7. Kinetic models (a) pseudo-first-order, (b) pseudo-second-order, and (c) intraparticle diffusion.

Table 2
Kinetic parameters

Pollutant	Pseudo-first-order				Pseudo-second-order				Intraparticle diffusion	
	K_1 (1/min)	q_e (mg/g)	Exp q_e (mg/g)	R^2	K_2 (g/mg min)	q_e (mg/g)	Exp q_e (mg/g)	R^2	R^2	k_i (mg/g min$^{0.5}$)
Phenol	0.0007	15.95	25.84	0.49	0.009	26.04	25.84	0.99	0.66	0.23
Pb	0.0007	11.39	25.76	0.5	0.032	25.9	25.76	1	0.31	0.13
Cr	0.0007	33.39	11.76	0.89	0.004	11.86	11.76	0.98	0.96	0.44
Cd	0.00002	37.39	2.64	0.04	0.1	2.66	2.64	0.98	0.13	0.04

Eq. (10), while enthalpy and entropy have been determined from the plot in Fig. 9d. It was observed from Table 3 that the free energy results for phenol and Pb at 30°C were negative, which indicates that the adsorption was spontaneous; however, the negativity decreased when the temperature was increased, which indicates that the adsorption condition became unfavorable [40]. However, for Cr(III) and Cd, the free energy was positive and decreased when the temperature was increased, which indicates a favorable condition since it is decreasing. Regarding enthalpy, for phenol, Pb, and Cd it was negative, which indicates that the adsorption was exothermic [40], however, for Cr(III), the enthalpy was positive, which indicates an endothermic reaction. The entropy value indicates the organization of the adsorbate in the solid-solution [40,41]. In the case of phenol, Pb, and Cd, the entropy where negative, which indicates that the adsorption is becoming less random, however, for Cr(III), the entropy is positive, which indicates

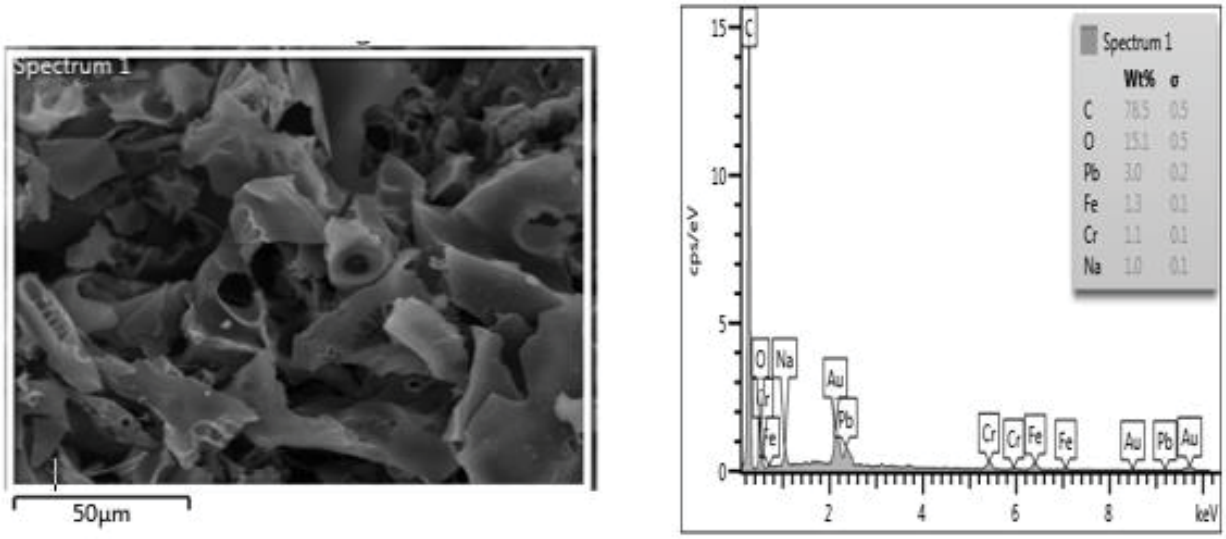

Fig. 8. SEM/EDS for the activated carbon after adsorption.

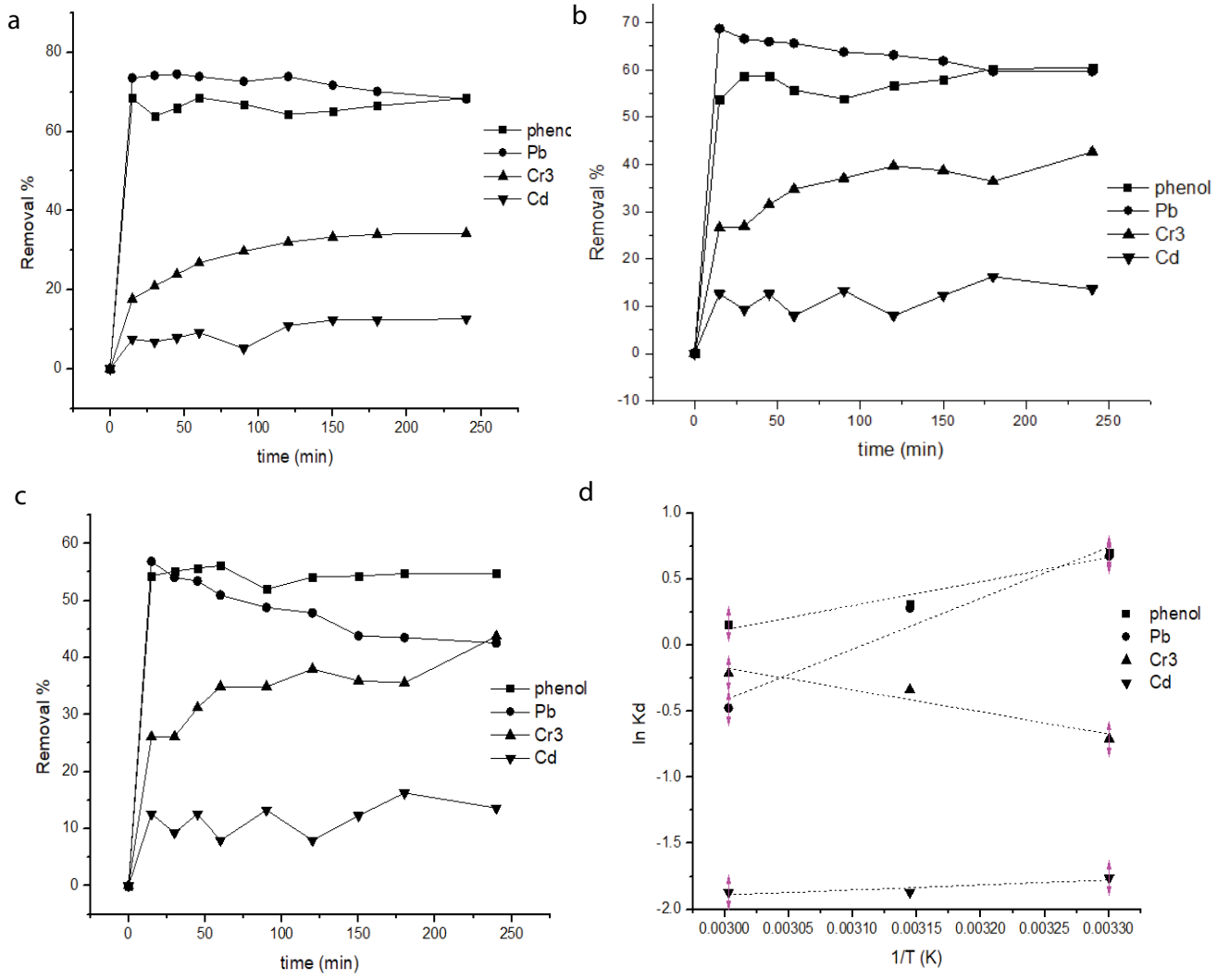

Fig. 9. Thermodynamic study (a) adsorption at 30°C, (b) adsorption at 45°C, (c) adsorption at 60°C, and (d) thermodynamic plot.

an increase in the randomness during the adsorption of Cr(III). Overall, the adsorption reaction was exothermic, which does not favor high-temperature conditions.

3.4. Regeneration

Chemical regeneration study has been done on the exhausted AC samples to examine the feasibility of the multiple reuses of the exhausted AC. Sodium hydroxide (NaOH) and hydrochloric acid (HCl) have been used due to their ability to weaken Van Der Waals's force [42]. The regeneration batch experiments were conducted at optimum conditions. The results of the removal efficiency of the initial run and three cycles can be found in Table 4. The recovery efficiency after three cycles was 81.4%, 29.7%, 47.8%, and 39% for phenol, Cr(III), Cd, and Pb, respectively, using NaOH. For HCl, the recovery efficiency was 59.5%, 58.6%, 79.4%, and 63.8% for phenol, Cr(III), Cd, and Pb, respectively. It can be observed from the adsorption–desorption cycle of the multicomponent system that using HCl was overall more effective than the use of NaOH on desorbing phenol with three metals. The use of NaOH obtained better results with phenol desorption because of the interaction between phenol and sodium that tends to dissociate phenol and create sodium salts, which assists in the desorption from the AC surface [24,43]. Rinkus et al. [44], who investigated the regeneration of phenol and Pb simultaneously using NaOH, reported that the regeneration performance was strongly affected by the NaOH concentration. In contrast, NaOH was weak in desorbing heavy metals and HCl obtained better results in removing metals from the AC surface. The HCl is a strong acid and that is why it eases the removal of metals from the AC surface by reducing the pH that causes an increase in the hydrogen ions that tend to compete with the adsorbed metal ions [45]. Anirudhan and Sreekumari [46], who investigated the desorption of heavy metals using HCl reported similar results. They reported that the hydrogen ions created by adding HCl contributed effectively in removing heavy metal ions attached to the activated carbon.

4. Conclusions

Mangrove charcoal activated using KOH was utilized in the batch adsorption experiments of phenol, Pb, Cr(III), and Cd in a multicomponent system. The results showed that the system was heavily influenced by the pH through the adsorption process, except for phenol, where the effect was minimal. Adsorbent dosage was also an important parameter, where the increase in the AC dosage caused an increase in the removal efficiency. The adsorption in the multicomponent system was unstable for phenol and Pb due to the competition on the AC surface and the interaction with the carbonyl group. The AC showed fluctuated affinity towards phenol and Pb based on the different operational parameters, sometimes the phenol removal was higher, and sometimes Pb removal was higher. However, in general, the affinity was highest for phenol > Pb > Cr > Cd. Adsorption isotherms showed that Freundlich isotherm fitted phenol and Cd, Langmuir fitted Pb and Cr(III), and Redlich–Peterson fitted Cd. Pseudo-second-order well-fitted data, which indicates that the adsorption is chemisorption. Intraparticle diffusion showed that the adsorption of phenol, Pb, and Cd occurred at two stages, while Cr(III) occurred at the macro level only in the multicomponent adsorption. The thermodynamic study showed that the adsorption was exothermic in nature. Finally, the regeneration study showed that it is very difficult to chemically regenerate the AC in a multicomponent system, because alkali treatment was good for phenol desorption and weak for heavy metals desorption, while acid treatment was good for heavy metal desorption and bad for phenol, however,

Table 3
Thermodynamic parameters

Pollutant	ΔG (J/mol)			ΔH (kJ/mol)	ΔS (J/K mol)
	30°C	45°C	60°C		
Phenol	–1,761.27	–831.67	–443.92	–15.16	–44.48
Pb	–1,708.4	–745.17	1,316.24	–32.08	–99.68
Cr	1,784.01	889.58	592.88	13.91	40.33
Cd	4,436.17	4,948.76	5,182.2	–3.15	25.16

Table 4
Desorption data

NaOH	Multicomponent				HCl	Multicomponent			
Pollutant	Phenol %	Cr %	Cd %	Pb %	Pollutant	Phenol %	Cr %	Cd %	Pb %
Initial	69.7	31.3	14	73.3	Initial	69.2	30.7	18	71
Cycle1	69.5	22.3	9.6	68	Cycle1	54.3	26	17.3	62.3
Cycle 2	67	21.3	7.2	44.3	Cycle 2	48.6	19.7	16.1	47.6
Cycle 3	56.8	9.3	6.7	28.6	Cycle 3	41.2	18	14.3	45.3

the overall results showed that HCl was better for the multicomponent system desorption.

Acknowledgment

The authors would like to express their gratitude to King Fahd University of Petroleum & Minerals (Dhahran, Saudi Arabia) for the technical and financial supports that were provided during the investigation.

References

[1] P.B. Tchounwou, C.G. Yedjou, A.K. Patlolla, D.J. Sutton, Heavy Metal Toxicity and the Environment, A. Luch, Ed., Molecular, Clinical and Environmental Toxicology, Experientia Supplementum, Vol. 101, Springer, Basel, 2012, pp. 133–164.
[2] P.K. Gautam, R.K. Gautam, S. Banerjee, M.C. Chattopadhyaya, J.D. Pandey, Chapter 4 – Heavy Metals in the Environment: Fate, Transport, Toxicity and Remediation Technologies, D. Pathania, Ed., Heavy Metals: Sources Toxicity and Remediation Techniques, Nova Science Publishers, New York, USA, 2016, pp. 101–130.
[3] H.R. Shamsollahi, M. Alimohammadi, S. Momeni, K. Naddafi, R. Nabizadeh, F.C. Khorasgani, M. Masinaei, M. Yousefi, Assessment of the health risk induced by accumulated heavy metals from anaerobic digestion of biological sludge of the lettuce, Biol. Trace Elem. Res., 188 (2019) 514–520.
[4] J.E. Emurotu, P.C. Onianwa, Bioaccumulation of heavy metals in soil and selected food crops cultivated in Kogi State, North Central Nigeria, Environ. Syst. Res., 188 (2019) 514–520.
[5] G. Issabayeva, S.Y. Hang, M.C. Wong, M.K. Aroua, A review on the adsorption of phenols from wastewater onto diverse groups of adsorbents, Rev. Chem. Eng., 34 (2018), doi: 10.1515/revce-2017–0007.
[6] A. Azari, M. Yeganeh, M. Gholami, M. Salari, The superior adsorption capacity of 2,4-dinitrophenol under ultrasound-assisted magnetic adsorption system: modeling and process optimization by central composite design, J. Hazard. Mater., 418 (2021) 126348, doi: 10.1016/j.jhazmat.2021.126348.
[7] W. Raza, J. Lee, N. Raza, Y. Luo, K.-H. Kim, J. Yang, Removal of phenolic compounds from industrial waste water based on membrane-based technologies, J. Ind. Eng. Chem., 71 (2019) 1–18.
[8] Y. Rashtbari, S. Hazrati, A. Azari, S. Afshin, M. Fazlzadeh, M. Vosoughi, A novel, eco-friendly and green synthesis of PPAC-ZnO and PPAC-nZVI nanocomposite using pomegranate peel: cephalexin adsorption experiments, mechanisms, isotherms and kinetics, Adv. Powder Technol., 31 (2020) 1612–1623.
[9] T.S. Hui, M.A.A. Zaini, Potassium hydroxide activation of activated carbon: a commentary, Carbon Lett., 16 (2015) 275–280.
[10] B. Buczek, Preparation of active carbon by additional activation with potassium hydroxide and characterization of their properties, Adv. Mater. Sci. Eng., 2016 (2016) 5819208, doi: 10.1155/2016/5819208.
[11] Paryanto, W.A. Wibowo, D. Hantoko, M.E. Saputro, Preparation of activated carbon from mangrove waste by KOH chemical activation, IOP Conf. Ser.: Mater. Sci. Eng., 543 (2019) 012087, doi: 10.1088/1757-899X/543/1/012087.
[12] R. Qadeer, N. Khalid, Removal of cadmium from aqueous solutions by activated charcoal, Sep. Sci. Technol., 40 (2005) 845–859.
[13] B. Devi, A. Jahagirdar, M. Ahmed, Adsorption of chromium on activated carbon prepared from coconut shell, Adsorption, 2 (2012) 364–370.
[14] A. Pal, H.-S. Kil, S. Mitra, K. Thu, B.B. Saha, S.-H. Yoon, J. Miyawaki, T. Miyazaki, S. Koyama, Ethanol adsorption uptake and kinetics onto waste palm trunk and mangrove based activated carbons, Appl. Therm. Eng., 122 (2017) 389–397.
[15] F. Ngugi, J.M. Onyari, J.N. Wabomba, Efficacy of mangrove (*Rhizophora mucronata*) roots powder in adsorption of lead(II) ions from aqueous solutions: equilibrium and kinetics studies, IOSR J. Appl. Chem., 9 (2016) 45–51.
[16] C.W. Oo, M.J. Kassim, A. Pizzi, Characterization and performance of *Rhizophora apiculata* mangrove polyflavonoid tannins in the adsorption of copper(II) and lead(II), Ind. Crops Prod., 30 (2009) 152–161.
[17] J. Anwar, U. Shafique, Waheed-uz-Zaman, M. Salman, A. Dar, S. Anwar, Removal of Pb(II) and Cd(II) from water by adsorption on peels of banana, Bioresour. Technol., 101 (2010) 1752–1755.
[18] N.F. Fahim, B.N. Barsoum, A.E. Eid, M.S. Khalil, Removal of chromium(III) from tannery wastewater using activated carbon from sugar industrial waste, J. Hazard. Mater., 136 (2006) 303–309.
[19] N. Ayawei, A.N. Ebelegi, D. Wankasi, Modelling and interpretation of adsorption isotherms, J. Chem., 2017 (2017) 3039817, doi: 10.1155/2017/3039817.
[20] S.M. Yakout, E. Elsherif, Batch kinetics, isotherm and thermodynamic studies of adsorption of strontium from aqueous solutions onto low cost rice-straw based carbons, Carbon – Sci. Technol., 3 (2010) 144–153.
[21] Z. Wang, Y. Jiang, X. Mo, X. Gu, W. Li, Speciation transformation of Pb during palygorskite sorption-calcination process: implications for Pb sequestration, Appl. Geochem., 124 (2021) 104850, doi: 10.1016/j.apgeochem.2020.104850.
[22] J. Liu, X. Wu, Y. Hu, C. Dai, Q. Peng, D. Liang, Effects of Cu(II) on the adsorption behaviors of Cr(III) and Cr(VI) onto kaolin, J. Chem., 2016 (2016) 3069754, doi: 10.1155/2016/3069754.
[23] U. Beker, B. Ganbold, H. Dertli, D.D. Gülbayir, Adsorption of phenol by activated carbon: influence of activation methods and solution pH, Energy Convers. Manage., 51 (2010) 235–240.
[24] B. Xie, J. Qin, S. Wang, X. Li, H. Sun, W. Chen, Adsorption of phenol on commercial activated carbons: modelling and interpretation, Int. J. Environ. Res. Public Health, 17 (2020) 789, doi: 10.3390/ijerph17030789.
[25] S.Z. Mohammadi, M.A. Karimi, D. Afzali, F. Mansouri, Removal of Pb(II) from aqueous solutions using activated carbon from sea-buckthorn stones by chemical activation, Desalination, 262 (2010) 86–93.
[26] N. Bouchelkia, L. Mouni, L. Belkhiri, A. Bouzaza, J.C. Bollinger, K. Madani, F. Dahmoune, Removal of lead(II) from water using activated carbon developed from jujube stones, a low-cost sorbent, Sep. Sci. Technol., 51 (2016) 1645–1653.
[27] E.-W.A. Abou El-Maaty, Removal of lead from aqueous solution on activated carbon and modified activated carbon prepared from dried water hyacinth plant, J. Anal. Bioanal. Technol., 5 (2014) 1000187, doi: 10.4172/2155-9872.1000187.
[28] M.H. Al-Malack, M. Dauda, Competitive adsorption of cadmium and phenol on activated carbon produced from municipal sludge, J. Environ. Chem. Eng., 5 (2017) 2718–2729.
[29] J.A. Arcibar-Orozco, J.R. Rangel-Mendez, P.E. Diaz-Flores, Simultaneous adsorption of Pb(II)-Cd(II), Pb(II)-phenol, and Cd(II)-phenol by activated carbon cloth in aqueous solution, Water Air Soil Pollut., 226 (2015) 2197, doi: 10.1007/s11270-014-2197-1.
[30] H.S. Mohamed, N.K. Soliman, D.A. Abdelrheem, A.A. Ramadan, A.H. Elghandour, S.A. Ahmed, Adsorption of Cd^{2+} and Cr^{3+} ions from aqueous solutions by using residue of *Padina gymnospora* waste as promising low-cost adsorbent, Heliyon, 5 (2019) e01287, doi: 10.1016/j.heliyon.2019.e01287.
[31] A. Alemu, B. Lemma, N. Gabbiye, K.Y. Foo, Adsorption of chromium(III) from aqueous solution using vesicular basalt rock, Cogent Environ. Sci., 5 (2019) 1650416, doi: 10.1080/23311843.2019.1650416.
[32] C. Faur-Brasquet, K. Kadirvelu, P. Le Cloirec, Removal of metal ions from aqueous solution by adsorption onto activated carbon cloths: adsorption competition with organic matter, Carbon N. Y., 40 (2002) 2387–2392.
[33] C. Moreno-Castilla, M.A. Álvarez-Merino, M.V. López-Ramón, J. Rivera-Utrilla, Cadmium ion adsorption on different carbon adsorbents from aqueous solutions. Effect of surface chemistry, pore texture, ionic strength, and dissolved natural organic matter, Langmuir, 20 (2004) 8142–8148.
[34] A.A. Basaleh, M.H. Al-Malack, T.A. Saleh, Methylene blue removal using polyamide-vermiculite nanocomposites:

kinetics, equilibrium and thermodynamic study, J. Environ. Chem. Eng., 7 (2019) 103107, doi: 10.1016/j.jece.2019.103107.
[35] W. Zhu, W. Yao, Y. Zhan, Y. Gu, Phenol removal from aqueous solution by adsorption onto solidified landfilled sewage sludge and its modified sludges, J. Mater. Cycles Waste Manage., 17 (2015) 798–807.
[36] M. Karnib, A. Kabbani, H. Holail, Z. Olama, Heavy metals removal using activated carbon, silica and silica activated carbon composite, Energy Procedia, 50 (2014) 113–120.
[37] C. Duan, T. Ma, J. Wang, Y. Zhou, Removal of heavy metals from aqueous solution using carbon-based adsorbents: a review, J. Water Process Eng., 37 (2020) 101339, doi: 10.1016/j.jwpe.2020.101339.
[38] Y. Fu, Y. Shen, Z. Zhang, X. Ge, M. Chen, Activated bio-chars derived from rice husk via one- and two-step KOH-catalyzed pyrolysis for phenol adsorption, Sci. Total Environ., 646 (2019) 1567–1577.
[39] C. Valderrama, X. Gamisans, X. de las Heras, A. Farrán, J.L. Cortina, Sorption kinetics of polycyclic aromatic hydrocarbons removal using granular activated carbon: intraparticle diffusion coefficients, J. Hazard. Mater., 157 (2008) 386–396.
[40] N.G. Rincón-Silva, J.C. Moreno-Piraján, L.G. Giraldo, Thermodynamic study of adsorption of phenol, 4-chlorophenol, and 4-nitrophenol on activated carbon obtained from eucalyptus seed, J. Chem., 2015 (2015) 569403, doi: 10.1155/2015/569403.
[41] M.A. Ahmad, N.A. Ahmad Puad, O.S. Bello, Kinetic, equilibrium and thermodynamic studies of synthetic dye removal using pomegranate peel activated carbon prepared by microwave-induced KOH activation, Water Resour. Ind., 6 (2014) 18–35.
[42] R. Berenguer, J.P. Marco-Lozar, C. Quijada, D. Cazorla-Amorós, E. Morallón, Electrochemical regeneration and porosity recovery of phenol-saturated granular activated carbon in an alkaline medium, Carbon N.Y., 48 (2010) 2734–2745.
[43] B. Özkaya, Adsorption and desorption of phenol on activated carbon and a comparison of isotherm models, J. Hazard. Mater., 129 (2006) 158–163.
[44] K. Rinkus, B.E. Reed, W. Lin, NaOH regeneration of Pb and phenol-laden activated carbon. I. Batch study results, Sep. Sci. Technol., 32 (1997) 2367–2384.
[45] T.D. Šoštarić, M.S. Petrović, F.T. Pastor, D.R. Lončarević, J.T. Petrović, J.V. Milojković, M.D. Stojanović, Study of heavy metals biosorption on native and alkali-treated apricot shells and its application in wastewater treatment, J. Mol. Liq., 259 (2018) 340–349.
[46] T.S. Anirudhan, S.S. Sreekumari, Adsorptive removal of heavy metal ions from industrial effluents using activated carbon derived from waste coconut buttons, J. Environ. Sci., 23 (2011) 1989–1998.

Supplementary information

The removal of phenol, Pb, Cd, Cr3 in singular solution with the following parameters: pH 5, dosage 1.25 g/L, and an initial concentration of 50 mg/L can be found in Fig. S1.

The Fourier-transform infrared spectroscopy in Figure S2 and Tables S1, S2 and the porosity analysis data of the used activated carbon can be found.

Table S1
Fourier-transform infrared spectroscopy data

Band and peak position	Functional groups/compounds
459.94–400	Aryl disulfides S–S
1,101.84	Secondary alcohol stretch C–O
1,556	Carbonyl group
1,614.42	Olefinic
2,358.04	C≡C
2,851–2,921.32	C–H stretching methyl and methylene group, or aliphatic group
3,442.95–3,700	OH stretching bond, N–H amine

Table S2
Surface and porosity data

Parameter	KOH activated carbon
Surface area (m^2/g)	784.29
Brunauer–Emmett–Teller surface area (m^2/g)	716.85
Micropore area (m^2/g)	546.52
External area (m^2/g)	170.33
Pore volume (cm^3/g)	0.45
Micropore volume (cm^3/g)	0.32
Pore size (nm)	2.5

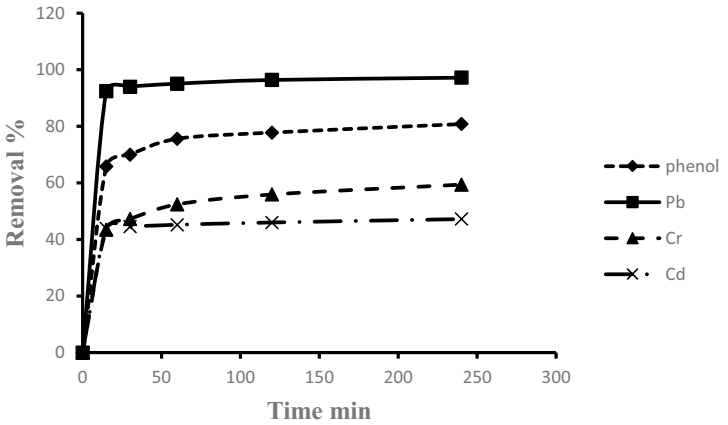

Fig. S1. Adsorption of phenol, Pb, Cr, and Cd in a singular adsorption system.

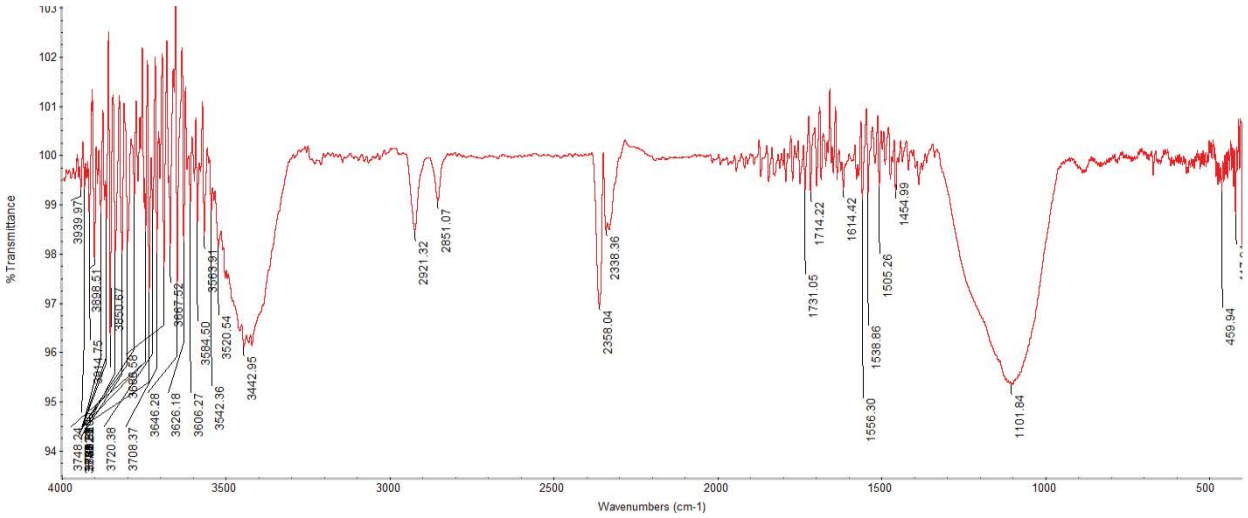

Fig. S2. Fourier-transform infrared spectroscopy for KOH-activated carbon.